論文 84-21-2-11

Numerical Analysis of a Two-Dimensional N-P-N Bipolar Transistor-BIPOLE

(2차원 N-P-N 바이폴라 트랜지스터의 수치해석-BIPOLE)

李 鍾 和*

(Jong Hwa Lee)

要 約

2차원 n-p-n 바이폴라 트랜지스터의 수치해석을 위한 프로그램(BIPOLE)을 개발하였다. 이 프로그램은 SRH와 Auger재결합 기구들과 불순물 농도와 전계강도에 대한 운송자 이동도의 의존성과 밴드 갭 축소 효과들을 포함하고 있다. Poisson 방정식에는 Newton법을 또 정공과 전자의 연속 방정식에는 발산이론을 이용하여 여러가지 물리적인 제한없이 기본 반도체 방정식들에 대한 유한차분 공식들을 만들었다. 선형화된 방정식들의 계수 행렬은 희소 대칭 M 행렬이었는데 그 해를 구하기 위해 ICCG법과 Gummel의 알고리즘을 적용하였다. 이 프로그램 BIPOLE를 n-p-n 트랜지스터의 여러가지 정상 상태 문제에 적용시켰다. 그 응용의 보기로서 공통 에미터 전류이득의 변화, 에미터 용량에 대한 확산용량이 미치는 영향과 입출력 특성곡선들을 계산해 보았다. 전위 분포와 전자와 정공 농도분포와 같은 계산 결과를 3차원 컴퓨터 그래픽으로 도시하였다. 이 프로그램은 장차 2차원 트랜지스터의 교류 및 왜곡 현상의 수치해석의 기초로 이용될 것이며, 이 프로그램에 관심있는 모든 분들께 공급될 것이다.

Abstract

A programme, called BIPOLE, for the numerical analysis of two-dimensional n-p-n bipolar transistors was developed. It has included the SRH and Auger recombination processes, the mobility dependence on the impurity density and the electric field, and the band-gap narrowing effect.

The finite difference equations of the fundamental semiconductor equations are formulated using Newton's method for Poisson's equation and the divergence theorem for the hole and electron continuity equations without physical restrictions.

The matrix of the linearized equations is sparse, symmetric M-matrix. For the solution of the linearized equations ICCG method and Gummel's algorithm have been employed.

The programme BIPOLE has been applied to various kinds of the steady-state problems of n-p-n transistors. For the examples of applications the variations of common emitter current gain, emitter and diffusion capacitances, and input and output characteristics are calculated. Three-dimensional representations of some D.C. physical quantities such as potential and charge carrier distributions were displayed. This programme will be used for the numerical analysis of the distortion phenomena of two-dimensional n-p-n transistors. The BIPOLE programme is available for everyone.

*正會員, 蔚山工科大學 材料工學科

(Dept. of Materials Science, Ulsan Institute of Technology)

接受日字 : 1984年 2月 3日

(※ 本 論文은 1983年度 蔚山工科大學의 現代研究費에 依하여 研究되었음.)

I. Introduction

The rigorous numerical modelling approach is a powerful tool for the description of bipolar transistors and for the optimization of process design without the conventional restrictions. This solution method was developed and

applied for the first time by Gummel.[1] Since then a number of authors extended the Gummel's one-dimensional iterative method to two-dimensional porblems and improved the finite difference method for the application to various semiconductor devices.[2]-[4]

De Mari,[5] for example, simulated the static and dynamic operation of the p-n diode, Tomizawa[6] developed a simulator for two dimensional bipolar transistors, Kennedy[7] studied with the JFET, and Selberherr[8] attempted a two-dimensional calculation for the MOS transistor.

For the two-dimensional analysis of silicon n-p-n transistors Heimeier[9,10] described a very efficient method. However, he did not include the high doping effect in his model.

Today the very large scale integration (VLSI) is a sophisticated technology which absolutely requires computer aided simulation of its devices. Especially because of the advancing rate of miniaturization one is compelled to use numerical models with increased accuracy and without fundamental physical restrictions.

In this work a computer programme was developed, called BIPOLE; a programme aimed at consistent numerical simulation of bipolar transistors. It will be used for the numerical analysis of the distortion and a.c. problems of bipolar transistors in the near future.

Three-dimensional computer graphics of some D.C. physical quantities are represented. Some applications are given for the purpose of demonstrating the use of BIPOLE.

II. The Physical Model

In order to accurately analyze a semiconductor structure under given circumstances, a system of the basic semiconductor equations must be solved, and in order to exactly model the system of equations only the inevitable assumptions for the mathematical descriptions of all the physical parameters and variables of the equations must be touched upon.

1. The Basic Semiconductor Equations

The fundamental semiconductor equations consist of Poisson's equation, continuity equations, and current equations.[11]

$$\text{div grad } \psi = -\frac{q}{\epsilon} \cdot (p-n+N) \tag{1}$$

$$\text{div } \bar{J}_n = q \cdot \frac{\partial n}{\partial t} + q \cdot R \tag{2}$$

$$\text{div } \bar{J}_p = -q \cdot \frac{\partial p}{\partial t} - q \cdot R \tag{3}$$

$$\bar{J}_n = q(-n \cdot \mu_n \cdot \text{grad}\psi + D_n \cdot \text{grad } n) \tag{4}$$

$$\bar{J}_p = q(-p \cdot \mu_p \cdot \text{grad}\psi - D_p \cdot \text{grad } p) \tag{5}$$

$$\bar{J} = \bar{J}_p + \bar{J}_n - \epsilon \cdot \frac{\partial}{\partial t} (\text{grad } \psi) \tag{6}$$

where all the symbols have their conventional meanings.

Almost all of the transport phenomena in a semiconductor device can be described in principle with this set of equations except only a few effects, e.g., the heat transfer phenomenon due to power dissipation and the degeneracy phenomenon due to high doping.

2. The Assumptions

For the exact numerical analysis of a semiconductor device only the inevitable assumptions have to be touched upon. However, some assumptions in the present work might significantly simplify the solution of the equations without a considerable loss of accuracy, and improve the computational speed.

Some important assumptions which have been established in the present work are as follows.

i) Only steady-state solutions are sought. This assumption significantly reduces the order of the partial differential equations and changes the finite difference equation formulation. By way of the suppression of the time dependent terms (i.e. $\frac{\partial p}{\partial t} = 0, \frac{\partial n}{\partial t} = 0$, and $\frac{\partial(\text{grad}\psi)}{\partial t} = 0$) a parabolic problem is converted to an elliptic problem.

ii) The total ionization of the donor and acceptor impurities will be assumed, i.e.,

$$N = N_D^+ - N_A^- = N_D - N_A \tag{7}$$

iii) The operating temperature throughout the

entire transistor is constant and assumed to be equal 300°K. All the physical parameters, therefore, are quoted the values at 300°K.

iv) The electron temperature is assumed to be equal to the crystal lattice temperature. The hot electron effect is neglected.

v) The heavy doping and degeneracy effects will be considered only by the effective intrinsic carrier density(n_{ie}). By way of this assumption and of the neglection of the asymmetric between conduction and valence bands the carrier distribution will be described by Boltzmann statistics.

$$n = n_{ie} \cdot \exp((\psi - \phi_n)/V_T) \tag{8}$$

$$p = n_{ie} \cdot \exp((\phi_p - \psi)/V_T) \tag{9}$$

vi) The Einstein relation is assumed to be valid.

$$D_n = \mu_n \cdot V_T \tag{10}$$

$$D_p = \mu_p \cdot V_T \tag{11}$$

vii) All the contacts are assumed to be ohmic. The space charge vanishes at the contacts, and the carrier distribution is in the thermal equilibrium. At all the other boundaries except the contacts the normal derivatives of potentials are considered to be zero and the normal component of the current density will vanish there. These assumptions will be used for the boundary conditions in the semiconductor device.

3. The Physical Parameters

The general basic semiconductor equations (1)-(6) contain several physical parameters of which the accuracy directly determines the quantitative validity of the total simulation results. The important physical parameters used in the present model are the carrier mobility; μ_n, μ_p, the net recombination rate; R, the effective intrinsic carrier density; n_{ie}, and the doping profile.

i) Mobilities: The mobility in general depends on several factors. The experimental dependence of carrier mobilities on doping density (N_t) and field strength($\bar{E}$) in silicon is well-described by Caughey and Thomas[12]. Their empirical formula for doping dependence of mobility is of the form;

$$\mu(N_t) = \frac{\mu_{max} - \mu_{min}}{1+(N_t/N_{ref})^a} + \mu_{min} \tag{12}$$

and the field dependence of mobility is as follows:

$$\mu(E) = \frac{\bar{V}}{\bar{E}} = \mu_o (1 + (E/E_c)^b)^{-1/b} \tag{13}$$

where $\mu_o = V_m/E_c$; zero-field mobility, and $N_t = |N_A| + |N_D|$

The best-fitting parameter values of these equations at room temperature are quoted from ref. [12].

A modified mobility relationship $\mu(N_t,E)$ is used in this work by assuming $\mu_o = \mu(N_t)$ and E_c to be a function of doping density, i.e., $E_c = V_m/\mu(N)$ and E_c to be a function of doping density, i.e., $Ec = V_m/\mu(N_t)$, treating V_m as a constant, then the mobility relationship is of the form;

$$\mu(N_t,E) = \frac{\mu(N_t)}{(1 + (\mu(N_t) \cdot |E|/V_m)^b)^{1/b}} \tag{14}$$

ii) Recombination rate: The dominant recombination-generation process in a silicon bipolar transistor is normally the Shockley-Read-Hall (R_{SRH}) recombination mechanism[13,14]. The Auger recombination mechanism will, however, be significant at highly doped region. The generation rate term due to the impact or avalanche ionization mechanism and band-to-band recombination terms are neglected in this work.

R_{SRH} model will be simplified by assuming the recombination centres to be in the middle of the energy gap as a single level. Then the simplest expression is written as follows:

$$R_{SRH} = \frac{nP - n_{ie}^2}{\tau_{po}(n+n_{ie}) + \tau_{no}(p+n_{ie})} \tag{15}$$

where n_{ie} is the effective intrinsic carrier concentration, the limiting lifetimes of the minority carrier; τ_{po} and τ_{no} are assumed

constant with the relation of $\tau_{po} = 0.2\,\tau_{no}$. Under the condition of low-level injection the Auger recombination mechanism can be written as follows;

$$R_{Auger} = C_p(np^2 - n_o p_o^2) + C_n(n^2 p - n_o^2 p_o) \simeq (C_n \cdot n + C_p \cdot p) \cdot (np - n_{ie}^2) \quad (16)$$

Net recombination rate is expressed by

$$R = R_{SRH} + R_{Auger} \quad (17)$$

iii) The effective intrinsic carrier density: The presence of the heavily doped impurities causes the semiconductor to behave as though its energy gap had been decreased by an amount ΔEg due to band edge tailing corresponding to a mobility band edge.

This bandgap narrowing effect causes the p-n product to increase as follows[15];

$$pn = n_{ie}^2(N_t, T) = n_i^2(T) \cdot \exp(q\Delta Vgo(N_t)/kT) \quad (18)$$

and the bandgap narrowing will be expressed by the following formula[15]

$$\Delta Vgo(N_t) = 9\times10^{-3} \cdot (\ln(N) + \sqrt{(\ln(N)^2 + 1/2)}) \ (V) \quad (19)$$

where $N = N_t/10^{17}$

iv) The doping profile: Typically, diffused layers are formed in a two-step process; predeposition and drive-in steps. The solution of Fick's second law in drive-in step takes well-known Gaussian distribution form.

The doping profile of two dimensional drive-in diffusion which is well described by Kennedy and O'Brien[16] takes the form;

$$C(x,y,t) = \frac{C_o}{4\sqrt{\pi Dt}} \cdot \exp\left(-\frac{y^2}{4Dt}\right) \cdot \left(1+\mathrm{erf}\left(\frac{x}{2\sqrt{Dt}}\right)\right) \quad (20)$$

where $C_o/\sqrt{\pi Dt}$ is the maximum surface concentration at y = 0, the last term denotes the diffusion parallel to the surface. In this work the parallel diffusion is approximated as a Gaussian distribution form.

The resulting Gaussian-type impurity distribution of the n-p-n transistor structure shown in Fig. 1 is given by

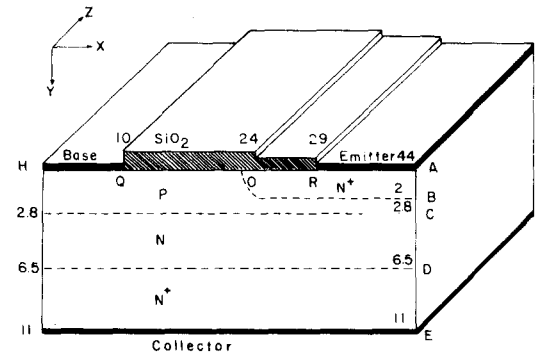

Fig. 1. The geometry of the n-p-n transistor investigated (Dimensions refer to micrometers).

$$N(x,y) = Ne(x,y) - N_b \cdot \exp(-C_2 \cdot y^2) + Nep + N_{bu} \cdot \exp(-C_1 \cdot (y-AE)^2) \quad (21)$$

where $Ne(x,y) = Ne \cdot \exp(-C_4 \cdot y^2)$ for $x \geq OH$

$Ne(x,y) = Ne \cdot \exp(-C_4 \cdot y^2) \cdot \exp(-C5 \cdot (OH-x)^2)$ for $x < OH$

Ne, N_b ; Emitter and base surface concentration

Nep ; Collector epitaxial layer doping density

N_{bu} ; Maximum buried layer impurity density

AE ; The emitter to collector distance

OH ; The emitter diffusion window edge

and C1 ; $\ln(N_{bu}/Nep)/(AE-AD)^2$

C2 ; $\ln(N_b/Nep)/AC^2$

C4 ; $(\ln(Ne) - \ln(N_b \cdot \exp(-C_2 \cdot AB^2) - Nep)/AB^2$

C5 ; $C_4/0.8$

These constants are obtained by putting the net impurity concentrations at the junctions to be zero.

Surface concentrations Ne, N_b, N_{bu} and the epitaxial layer concentration Nep as well as layer thicknesses and geometrical distances AB, AC, AD and AE are given as input data.

III. The Numerical Model

In order to transform a physical model of a semiconductor to a numerical model, the fundamental equations should be normalized for the simplicity of the equations. The normalized equations are linearized to be discretized. The recurrent finite difference equations are formulated from the differential equations with the applicable boundary conditions.

1. The Normalization of the Basic Equations

For the purpose of clarity and simplicity the set of semiconductor equations must be normalized by the appropriate normalization factors shown in ref. [17].

The final system of the normalized equations under the assumptions of chapter II is as follows;

$$\text{div}\cdot\text{grda}\ \psi = n\text{-}p\text{-}N \tag{22}$$

$$\text{div}\ \bar{J}_p = -R \tag{23}$$

$$\text{div}\ J_n = R \tag{24}$$

$$\bar{J}_n = -D_p\cdot n_{ie}\cdot\exp(-\psi)\cdot\text{grad}\ \Phi_p \tag{25}$$

$$\bar{J}_n = D_n\cdot n_{ie}\cdot\exp(\psi)\cdot\text{grad}\ \Phi_n \tag{26}$$

$$n = n_{ie}\cdot\exp(\psi)\cdot\psi_n \tag{27}$$

$$p = n_{ie}\cdot\exp(-\psi)\cdot\Phi_p \tag{28}$$

Φ_n and Φ_p are so-called Slotboom Variables,[18] which denote the exponential forms of electron and hole quasi-Fermi potentials; i.e.

$$\Phi_n = \exp(-\phi_n) \tag{29}$$

$$\Phi_p = \exp(\phi_p) \tag{30}$$

Three main variables to be solved are ψ, Φ_p, and Φ_n instead of ψ, ϕ_n, and ϕ_p.

2. The Discretization of Poisson's Equation

We assume that ψ is only δ off ψ exact

$$\psi\text{exact} = \psi+\delta \tag{31}$$

then Poisson's equation is approximated using Taylor series.

$$\text{div grad}\ \delta - (n+p)\cdot\delta = n\text{-}p\text{-}N - \text{div grad}\psi + o(\delta^2) \tag{32}$$

If we apply the central substitution for the second order derivatives of div grad terms, the finite difference equation of Poisson's equation may be written as follows;

$$A\delta_{i,j-1} + B\delta_{i-1,j} + C\delta_{i,j} + D\delta_{i+1,j} + E\delta_{i,j+1} = BB_{i,j} \tag{33}$$

where $A = -g_j\cdot H$, $\quad B = -h_i\cdot G$

$D = -h_i\cdot G$, $\quad E = -g_{j-1}\cdot H$

$C = (-A-B-D-E+n+p)\cdot G\cdot H$

$BB = (p\text{-}n+N-A\cdot\psi_{i,j-1}-B\cdot\psi_{i-i,j} + (A+B+D+E), \psi_{i,j}-D\cdot\psi_{i+i,j} \cdot -E\cdot\psi_{i,j+1})\cdot G\cdot H$

$$H = \frac{h_i + h_{i-1}}{2} \qquad G = \frac{g_j + g_{j-1}}{2}$$

3. The Discretization of the Continuity Equations

Before we consider the discretizations of continuity equations, we will use the Slotboom variables (Φ_p and Φ_n) to avoid the exponential nonlinearity of quasi-Fermi potentials, and change the net recombination rate R to solve the equations implicitly.

The net recombination rate R for the hole continuity equation can be approximated by the iternative solutions of mth and (m+1)th iterations.

$$R^{m+1} = R^m + \frac{\partial R}{\partial \Phi_p}\, d\Phi_p = R^m + R_p\cdot(\Phi_p^{m+1} - \Phi_p^m) \tag{34}$$

where $$R_p = \frac{\partial R}{\partial p}\cdot\frac{\partial P}{\partial \Phi_p} \tag{35}$$

and for the electron continuity equation

$$R^{m+1} = R^m + R_n\cdot(\Phi_n^{m+1} - \Phi_n^m) \tag{36}$$

where $$R_n = \frac{\partial R}{\partial n}\cdot\frac{\partial N}{\partial \Phi_n} \tag{37}$$

If the hole continuity equation is combined with the equation (34), then,

$$\text{div}\ \bar{J}_p = \text{div}(-D_p\cdot n_{ie}\cdot\exp(-\psi)\cdot\text{grad}\ \Phi_p^{m+1})$$

$$= -R^m + R_p\cdot\Phi_p^m - R_p\cdot\Phi_p^{m+1} \tag{38}$$

and if we take the volume integral at both sides of this equation :

$$\iiint \mathrm{div}\,(-D_p \cdot n_{ie} \cdot \exp(-\psi) \cdot \mathrm{grad}\,\Phi_p^{m+1})\,dx\,dy\,dz + \iiint R_p \cdot \Phi_p^{m+1}\,dx\,dy\,dz = \iiint F\,dx\,dy\,dz \quad (39)$$

where $F = -R^m + R_p \cdot \Phi_p^m$

Since all the variables are invariant along z-direction for two dimensional problem, the volume integrals can be changed to the surface intergrals;

$$\iint \mathrm{div}\,(-D_p \cdot n_{ie} \cdot \exp(-\psi) \cdot \mathrm{grad}\,\Phi_p^{m+1})\,dx\,dy + \iint R_p \cdot \Phi_p^{m+1}\,dx\,dy = \iint F\,dx\,dy \quad (40)$$

With the help of a divergence theorem and a Green-like theorem, the first surface intergral in the above equation can be transformed into a convolution line integral over the boundary of subregion as the rectangular dashed lines shown in Fig. 2.

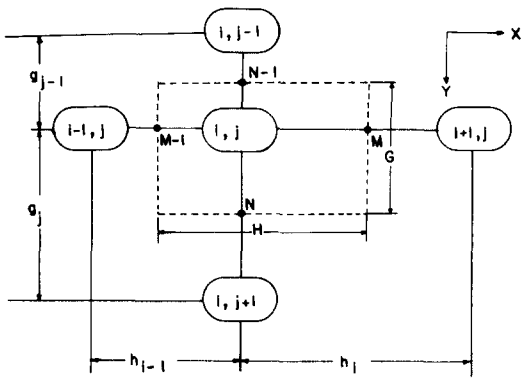

Fig. 2. Typical nodes for two-dimensional finite difference equation formulation (after ref. [8]).

$$\iint \mathrm{div}\,(-D_p \cdot n_{ie} \cdot \exp(-\psi) \cdot \mathrm{grad}\,\Phi_p)\,dx\,dy = -\oint \alpha_p \left(\frac{\partial \Phi}{\partial x} P \cdot dy + \frac{\partial \Phi_p}{\partial y} \cdot dx\right) \quad (41)$$

where $\alpha_p = D_p \cdot n_{ie} \cdot \exp(-\psi)$

$D_p \cdot n_{ie}$ may be considered almost constant between two neighbouring mesh points because D_p decreases and n_{ie} increases with increasing doping density, and $\exp(-\psi)$ can be expressed by Bernoulli function, then without subscript p of Φ_p and α_p the discretized form of this equation will be written as;

$$\oint \alpha \cdot \left(\frac{\partial \Phi}{\partial x}\,dy + \frac{\partial \Phi}{\partial y}\,dx\right) = G \cdot (\alpha_M \cdot (\Phi_{i+1,j} - \Phi_{i,j})/h_i + \alpha_{M-1} \cdot (\Phi_{i-1,j} - \Phi_{i,j})/h_{i-1}) + H \cdot (\alpha_N \cdot (\Phi_{i,j+1} - \Phi_{i,j})/g_i + \alpha_{N-1} \cdot (\Phi_{i,j-1} - \Phi_{i,j})/g_{j-1}) \quad (42)$$

Under the assumption that all the functions are smooth in the subregion, the second and third surface integrals of equation (40) can be discretized in a common way;

$$\iint F\,dx\,dy = F_{ij} \cdot G \cdot H \quad (43)$$

$$\iint R \cdot \Phi\,dx\,dy = R_{i,j} \cdot \Phi_{ij} \cdot G \cdot H \quad (44)$$

After combination of these discretized equations one obtains for each inner point (i, j) a finite difference equation for the hole continuity equation with the following form;

$$A\,\Phi_{i,j-1} + B\,\Phi_{i-1,j} + C\,\Phi_{i,j} + D\,\Phi_{i+1,j} + E\,\Phi_{i,j+1} = BB_{i,j} \quad (45)$$

where $A = -H \cdot \alpha_{N-1}/g_{j-1}$, $B = -G \cdot \alpha_{M-1}/h_{i-1}$
$D = -G \cdot \alpha_M/h_i$, $E = -H\,\alpha_N/g_j$
$C = -A - B - D - E + R_{pi,j} \cdot G \cdot H$
$BB_{i,j} = (-R^m + R_p \cdot \Phi^m) \cdot G \cdot H$

By the similar method one can obtain the finite difference equation for the electron continuity equation which is the same for the hole except the difinition of α_n and R_n

4. The Matrix Consideration and the Iterative Solution Method

We construct the equations for all of the grid points, which are linear in one set for

each basic equation, such that each basic equation can be presented in a linear matrix form.

$$Mx = P \tag{46}$$

Since the mesh is set up with NX·NY points we can see that the coefficient A of the (NX+1) st equation is equal to E of the first equation, similarly D of the 2nd equation equal to B of the 3rd equation, hence the resulting matrix is symmetric. Therefore only C, D and E elements and P pertinent vector will be calculated in the BIPOLE.

The matrix M is a sparse symmetric M-matrix where M-matrix means that a matrix $A=(a_{ij})$ is an M-matrix if $a_{ij} \leq 0$ for $i \neq j$, A is nonsingular and $A^{-1} V0$. In the equation (46) x represents an unknown vector (ψ, Φ_p, or Φ_n) with the length of (NX-2)·(NY-2). The matrix M in many practical two dimensional problems is of very high rank (NX-2), (NY-2). As the coefficient matrix of a set of equations it has five non-zero diagonally dominant elements in each row.

We will employ a special iterative solution method for the equation (46) by using the characteristics of this sparse symmetric M-matrix. The solution method is called ICCG[19] (Incomplete Choleski and Conjugate Gradient) method because it is based on the incomplete decomposition of matrix M; i.e. M=K−R and the use on conjugate gradient method for the acceleration of convergence rate.

5. The Boundary Conditions and the Grid Generation

In order to sufficiently bound the linearization and discretization error, we have to pay attention to the selection of the grid points. The grid spacing is chosen unequally by considering the doping density and electro-static potential.

The boundary conditions are based on the followings: The contacts will be assumed to be ohmic. The electrostatic potential will have the sum of the applied potential and the built-in potential due to the doping. The quasi-Fermi potentials for holes and electrons will be just the applied potentials, i.e., zero at the emitter contact, V_{BE} at the base and V_{CE} at the collector following the common emitter configuration. The hole and electorn imrefs will be equal at the contacts due to the assumption of the carrier equilibrium distribution.

All the boundary conditions for the n-p-n transistor with a common emitter configuration can be summarized as;

i) At the emitter contact

$$\phi_n = \phi_p = o, \qquad \psi = \ln(Ne/n_{ie})$$

ii) At the base contact

$$\phi_p = \phi_n = V_{BE}, \qquad \psi = V_{BE} - \ln(N_b/n_{ie})$$

iii) At the collector contact

$$\phi_p = \phi_n = V_{CE}, \qquad \psi = V_{CE} + \ln(N_{bu}/n_{ie})$$

iv) For the symmetric plane or oxide surface

$$\frac{\partial \phi_n}{\partial \bar{n}} = \frac{\partial \phi_p}{\partial \bar{n}} = \frac{\partial \psi}{\partial \bar{n}} = 0$$

where $\bar{n}$ is the normal direction coordinate at the boundary. This condition gives the normal components of $\bar{J}_p$ & $\bar{J}_n$ to be equal zero.

IV. Results and Applications

The programme BIPOLE developed in this work has been applied to various kinds of steady state and small signal low frequency problems of a bipolar n-p-n transistor structure with a few modifications. The computer graphics of D.C. quantities and the transitor characteristics curves are presented for the purpose of demonstrating the use of BIPOLE.

Fig. 3 shows the doping profile of the transistor structure shown in Fig. 1. The surface densities at the contacts are taken to be NE=1.55568E20, NB=3.11783E18, and NC=1.15E19. The impurity density of the epitaxial process Nep is taken to be 5.E16. The lateral impurity diffusion near the emitter diffusion mask was assumed 0.8 times normal diffusion constant.

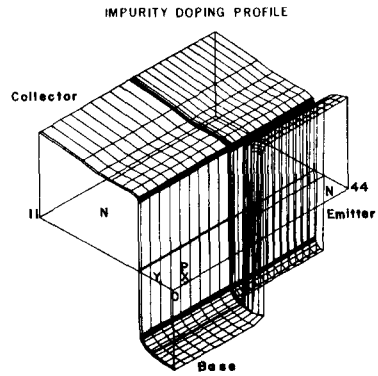

Fig. 3. Doping profile of the transistor with the surface concentrations NE= 1.55568E20, NB=3.11783E18, NC= 1.15E19, and epitaxial layer Nep= 5.0E16.

D.C. physical quantities have been obtained under a variety of bias conditions. The limiting lifetimes of the SRH-recombination process are taken to be 100 nsec for holes and 500 nsec for electrons.

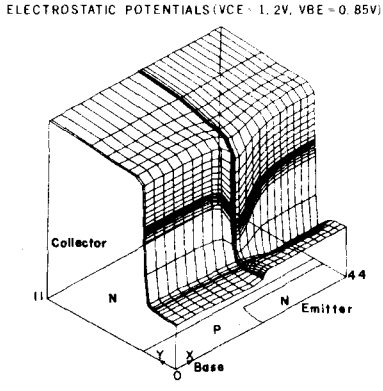

Fig. 4. Electrostatic potential distribution in the transistor under the bias condition VBE=0.85V and VCE=1.20V.

Fig. 4 shows the distribution of the electrostatic potential in the transistor under the bias conditions VBE=0.85V, VCE=1.20V. Small y-direction electrostatic potential gradient due to the collector resistance is observed at the neutral collector region. The x-direction electric field near the centre of collector region is also observed, causing x-direction currents to the centre. The potential gradient along the narrow active base region appears due to base resistance, which may cause a non-uniform emitter current density distribution. The highest electric field is located at the reverse biased base-collector junction, hence there is no Kirk effect observed under these bias conditions.

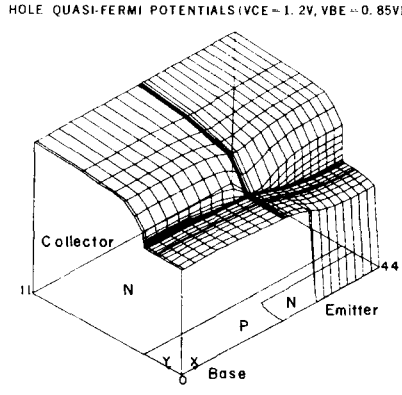

Fig. 5. Hole quasi-Fermi potential distribution in the transistor under the bias condition VBE=0.85V and VCE=1.20V.

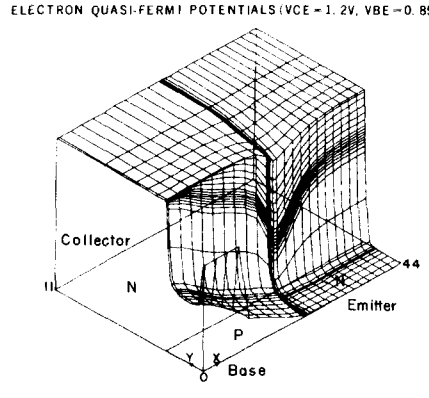

Fig. 6. Electron quasi-Fermi Potential distribution in the transistor under the bias condition VBE=0.85V and VCE= 1.20V.

Fig. 5 and 6 show hole and electron quasi-Fermi potential distributions under the same bias conditions. Electron quasi-Fermi potential is zero at the whole emitter region and nearly constant at the neutral collector region. It, however, rises steadily at the nonactive base

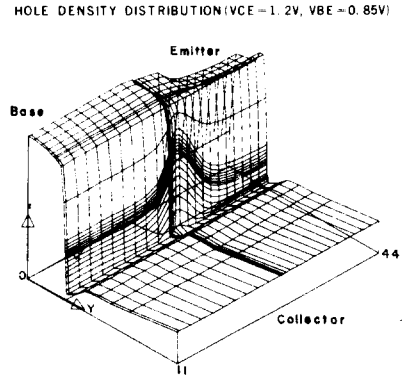

Fig. 7. Hole carrier density distribution in the transistor under the bias condition VBE=0.85 and VCE=1.20V.

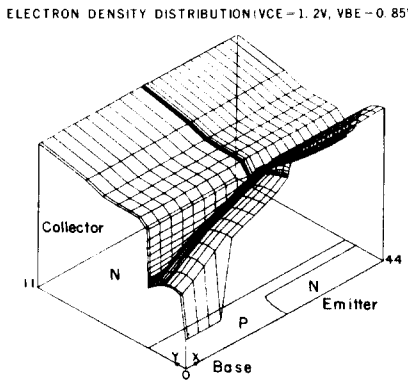

Fig. 8. Electron carrier density distribution in the transistor under the bias condition VBE=0.85V and VCE=1.20V.

region.

Fig. 7 and 8 show hole and electron concentration distributions. One can see the hole density injected from base to emitter and the electron density injected from emitter to base which are rather high-level injection. The hole concentration increases approximately linearly at the collector region. One can see the hole carrier minimum near the base-collector junction, representing the depletion region.

Fig. 9 is a semilog plot of calculated collector and base currents versus emitter-base voltage for VCE=1.0V. The knee current and knee voltage at which the effective emission

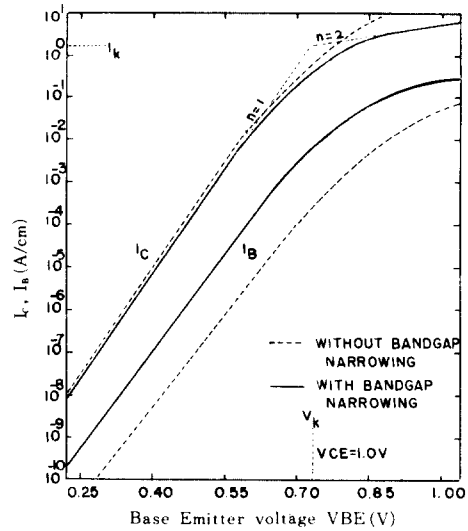

Fig. 9. Calculated collector and base currents versus base-emitter voltage for VCE= 1.0V.

coefficient n is changed from one to two are 1.26 A/cm and 0.73 volts. This knee voltage is quite similar to V_k=0.74V of ref. [20].

The relative importance of bandgap narrowing effect is also shown in Fig. 9 by comparing the currents with and without bandgap narrowing effect. Fig. 9 clearly shows that bandgap narrowing must be considered for accurate

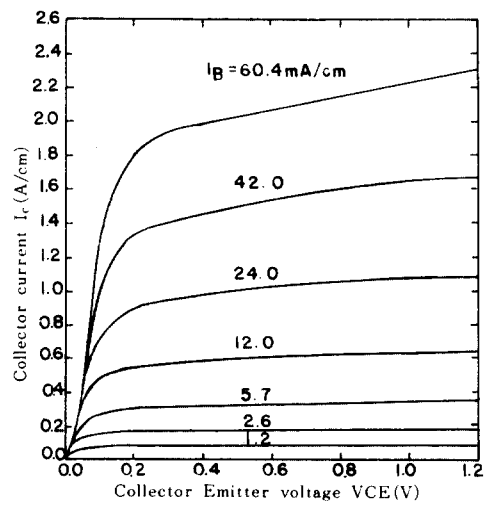

Fig.10. Calculated collector current versus collector emitter voltage with base current as the parameter.

current calculation. Without bandgap narrowing the base current is much underestimated and current gain will be overestimated.

Fig. 10 presents the calculated output characteristics for the transistor in common emitter configuration. The collector current of saturation region increases with increasing VCE (see I_B=60.4 mA/cm curve). This causes common emitter current gain to increase because of lack of the saturation phenomenon and decrease of the effective base width. One can calcuated the Early voltages V_A from the slopes of the curves. The calculated Early voltages for each curve are not equal because the effective base width is too narrow comparing with the depletion layer of base-collector junction. They appear 5.0, 5.7, 17.0 volts for I_B=60.4, 42.0, 5.7 mA/cm which correspond to VBE=0.85. 0.82, 0.73 volts.

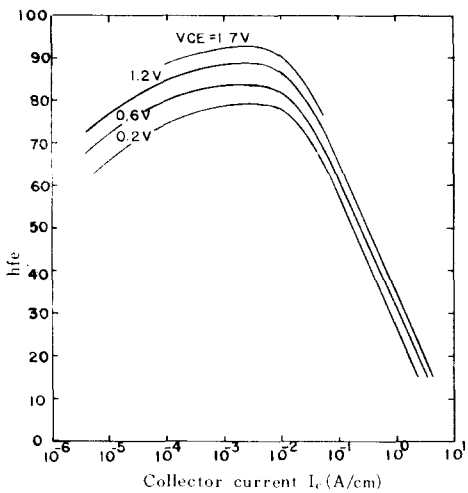

Fig.11. Calculated small signal low frequency current gain h_{fe} versus collector current for various collector-emitter voltages.

Fig. 11 shows the calculated common-emitter small signal low-frequency current gain versus collector current with the collector-emitter voltage as the parameter. One can see the current gain decreases linearly for higher collector current than 1.E-2 A/cm due to high-level injection effect.

Fig. 12 shows the diffusion capacitance

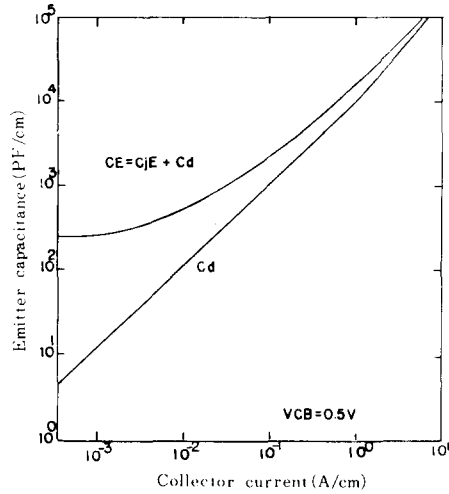

Fig.12. Calculated emitter and diffusion capacitances CE and Cd versus collector current for base-collector voltage 0.5V.

contribution to the emitter capacitance. As collector current increases higher than 2 A/cm the diffusion capacitance is dominant, thereby giving rise to injection current gain degradation.

V. Conclusion

A programme, called BIPOLE, for the numerical analysis of two-dimensional n-p-n bipolar transistors has been developed using the finite difference equations of the fundamental semiconductor equations without physical restrictions. This programme package includes the SRH and Auger recombination processes, the mobility dependences on the impurity atom density and the electric field strength, and the band-gap narrowing effect, but not surface and band-to-band direct recombinations.

The finite difference equation formulations for the basic semiconductor equations are fully explained. The resulting matrices of the linearized equations are sparse, symmetric M-materices. For the solution of the equations the ICCG method has been employed.

The programme BIPOLE has been applied to various kinds of the steady-state problems. Three-dimensional representations of some D.C.

Physical quantities such as potential and charge carrier distributions were displayed.

For the examples of applications, the static and small signal low frequency current gains, emitter and diffusion capacitances, and input and output characteristics are calculated.

Furthermore, it has also been made possible to obtain a deeper physical insight into the functioning of various kinds of device size and geometry. The author wish this programme should provide an interest and an academic exchange opportunity for the experienced semiconductor engineers and lecturers, and should appeal to the designers of devices and circuits with IC or discrete devices.

Acknowledgement

The Author would like to thank Dr. W. Fulop at the Brunel University, England for his invaluable advice and encouragement.

He is indebted to the computer centre of the Ulsan Institute of Technology for generously providing computer time. This work was supported by the Funds for the research of Hyundai.

References

[1] H.K. Gummel, "A self-consistent iterative scheme for one-dimensional steady state transistor calculations," *IEEE Trans. Electron Devices*, vol. ED-11, pp.455-465, 1964.

[2] S.C. Choo, "Numerical analysis of a forward-biased step-junction P-L-N diode," *IEEE Trans. Electron Devices*, vol. ED-18, pp.574-586, 1971.

[3] M.S. Mock, "On the convergence of Gummel's numerical algorithm," *Solid-State Electron.*, vol. 15, pp.1-4, 1972.

[4] M. Kurata, "Design considerations of step recovery diodes with the aid of numerical large-signal analysis," *IEEE Trans. Electron Devices*, vol. ED-19, pp.1207-1215, 1972.

[5] A. De Mari, "An accurate numerical one-dimensional solution of the P-N junction under arbitrary transient conditions," *Solid-State Electron.*, vol. 11, pp.1021-1053, 1968.

[6] M. Tomizawa, et al, "An accurate design method of bipolar devices using a two-dimensional device simulator," *IEEE Trans. Electron Devices*, vol. ED-28, pp.1148-1153, 1981.

[7] D.P. Kennedy and R.R. O'Brien, "Computer aided two-dimensional analysis of the junction field-effect transistor," *IBM J. Res. Develop.*, vol. 14, pp.95-116, 1970.

[8] S. Selberherr, Two-dimensional modeling of MOS transistors, Ph.D. thesis, Technical University of Vienna, Austria, 1982.

[9] H.H. Heimeier, "A two-dimensional numerical analysis of a silicon n-p-n transistor," *IEEE Trans. Electron Devices*, vol. ED-20, pp.708-714, 1973.

[10] O. Manck, H.H. Heimeier, and W.L. Engl, "High injection in a two-dimensional transistor," *IEEE Trans. Electron Devices*, vol. ED-21, pp.403-409, 1974.

[11] S.M. Sze, Physics of Semiconductor Devices, 2nd Ed, J. Wiley, New York, pp.50, 1981.

[12] D.M. Caughey and R.E. Thomas, "Carrier Mobilities in silicon empirically related to doping and field," *Proc. IEEE*, vol. 55, pp.2192-2193, 1967.

[13] W. Shockley and W.T. Read Jr., "Statistics of the recombinations of holes and electrons," *Physical Rev.*, vol. 87, pp.835-841, 1952.

[14] S.M. Sze, Ref. [11] pp.35.

[15] J.W. Slotboom, "The pn-product in silicon," *Solid-State Electron.*, vol. 20, pp.279-283, 1977.

[16] D.P. Kennedy and R.R. O'Brien, "Analysis of the impurity atom distribution near the diffusion mask for a planar p-n junction," *IBM J. Res. Develop.*, vol. 9, pp. 179-186, 1965.

[17] J.H. Lee, "A review of semiconductor numerical solution methods and two-

dimensional finite difference equation formulation for analysis of thyristors with shorted emitters," M.S. thesis, Brunel University, England, 1981.

[18] J.W. Slotboom, "Computer-aided two-dimensional analysis of bipolar transistors," *IEEE. Trans. Electron Devices*, vol. ED-20, pp.669-679, 1973.

[19] J.A. Meijerink and H.A. Van der Vorst, "An iterative method for linear systems of which the coefficient matrix is a symmertic M-Matrix," *Math. of Computation*, vol. 31, No. 137, pp.148-162, 1977.

[20] H.K. Gummel and H.C. Poon, "An integral charge control model of bipolar transistors," *Bell Sys. Tech. J.*, vol. 49, pp.827-851, 1970.